

An X-ray diffraction study of  $\text{Ni}_{(\text{aq})}^{2+}$  and  $\text{Mg}_{(\text{aq})}^{2+}$  by difference methods

This article has been downloaded from IOPscience. Please scroll down to see the full text article.

1989 J. Phys.: Condens. Matter 1 3489

(<http://iopscience.iop.org/0953-8984/1/22/009>)

View [the table of contents for this issue](#), or go to the [journal homepage](#) for more

Download details:

IP Address: 94.79.44.176

The article was downloaded on 10/05/2010 at 18:11

Please note that [terms and conditions apply](#).

## An x-ray diffraction study of $\text{Ni}_{[\text{aq}]}^{2+}$ and $\text{Mg}_{[\text{aq}]}^{2+}$ by difference methods

N T Skipper<sup>†</sup>, G W Neilson and S C Cummings<sup>‡</sup>

H H Wills Physics Laboratory, University of Bristol, Tyndall Avenue, Bristol BS8 1TL, UK

Received 10 October 1988, in final form 10 January 1989

**Abstract.** Difference methods of x-ray diffraction have been used to study the microscopic structure around  $\text{Ni}_{[\text{aq}]}^{2+}$  and  $\text{Mg}_{[\text{aq}]}^{2+}$  in a variety of aqueous solutions. Reference to the results of neutron diffraction experiments has shown that  $\text{Ni}_{[\text{aq}]}^{2+}$  and  $\text{Mg}_{[\text{aq}]}^{2+}$  can be regarded as structurally isomorphic species, thereby enabling the local ionic structure to be measured in terms of the cation–oxygen and cation–cation radial pair distribution functions,  $g_{\text{MO}}(r)$  and  $g_{\text{MM}}(r)$ . Results are included for the dependence of these functions on concentration, counter-ion species and the interchange of light and heavy water as the solvent.

### 1. Introduction

One of the most intractable problems in the study of aqueous electrolyte solutions is the experimental determination of ion–ion distribution functions. In certain favourable cases this information can be derived from the second-order difference method of neutron diffraction. However, these experiments are at the limit of present technology, because the contributions to the total diffraction pattern from the ion–ion terms are small. We have therefore developed a new technique, based on isomorphic substitution and x-ray diffraction, for which the weightings of the ion–ion terms are larger.

A preliminary account of this work has already been published (Skipper *et al* 1986), and we now give fuller details of the method. We also include new results, some of which are complementary to those obtained from earlier neutron diffraction experiments, and some of which demonstrate that at the level of a second-order difference the x-ray method can surpass the neutron method.

### 2. Theoretical background

#### 2.1. Diffraction from aqueous solutions

The basic structure of an aqueous electrolyte solution,  $\text{MX}_n$  in  $\text{H}_2\text{O}$ , can be written in terms of ten radial pair distribution functions,  $g_{\alpha\beta}(r)$ . Of these,  $g_{\text{HH}}(r)$ ,  $g_{\text{HO}}(r)$  and  $g_{\text{OO}}(r)$  describe the water structure,  $g_{\text{MM}}(r)$ ,  $g_{\text{MX}}(r)$  and  $g_{\text{XX}}(r)$  describe the ionic structure, and

<sup>†</sup> Department of Earth Sciences, University of Oxford, UK

<sup>‡</sup> Schuster Physics Laboratory, University of Manchester, UK

$g_{MO}(r)$ ,  $g_{MH}(r)$ ,  $g_{XO}(r)$  and  $g_{XH}(r)$  describe the ion–water structure. These functions can be related to the x-ray or neutron structure factors of the sample,  $F_X(k)$  or  $F_N(k)$ , which can be obtained from the experimental intensity,  $I(k)$ ;

$$F(k) = \alpha(k)[I(k) + \gamma(k)] \quad (1)$$

where  $k = (4\pi/\lambda) \sin \theta$  is the scattering wavenumber,  $\hbar k$  is the momentum transfer of x-rays or neutrons of wavelength  $\lambda$ , scattered through an angle  $2\theta$ , and  $\alpha(k)$  and  $\gamma(k)$  represent correction functions which must be used to obtain a properly normalised structure factor (Enderby and Neilson 1981).  $F(k)$  can be written as

$$F(k) = \sum_{\alpha} \sum_{\beta} c_{\alpha} c_{\beta} f_{\alpha}(k) f_{\beta}(k) [S_{\alpha\beta}(k) - 1] \quad (2)$$

where  $f_{\alpha}(k)$  is either the x-ray form factor of species  $\alpha$  or the neutron scattering length of nucleus  $\alpha$ .  $c_{\alpha}$  is the atomic fraction of scattering centres  $\alpha$ , and the sums are over all scattering species.  $S_{\alpha\beta}(k)$  is the partial structure factor of species  $\alpha$  and  $\beta$ , which can be related to  $g_{\alpha\beta}(r)$  by Fourier transformation;

$$g_{\alpha\beta}(r) - 1 = 1/(2\pi^2\rho r) \int_0^{\infty} [S_{\alpha\beta}(k) - 1] \sin(kr) k dk \quad (3)$$

where  $\rho$  is the total number density of particles in the system, and is typically  $0.1 \text{ \AA}^{-3}$  for an aqueous solution.

Since ten partial structure factors contribute to the total structure factor of an aqueous electrolyte solution, it is difficult to obtain unambiguous structural information concerning the ions from a single diffraction experiment (Neilson and Enderby 1979). This situation can be improved by the use of difference techniques.

## 2.2. Difference methods in diffraction experiments

The difference method of neutron diffraction based on isotopic substitution has been discussed elsewhere (Soper *et al* 1977), and we will only point out the important results here. Briefly, it is possible to carry out sets of neutron diffraction experiments on isotopically distinct samples and thereby obtain detailed structural information concerning the environment around the substituted species. There are two levels at which this can be done. The first is at the ion–solvent level, and leads to a first-order difference distribution function,  $G_M(r)$ . Taking the example of cation (M) substitution;

$$G_M(r) = Ag_{MO}(r) + Bg_{MD}(r) + Cg_{MX}(r) + Dg_{MM}(r) + E \quad (4)$$

where  $A = 2c_O c_M f_O (f_M - f_{M'})$ ,  $B = 2c_D c_M f_D (f_M - f_{M'})$ ,  $C = 2c_X c_M f_X (f_M - f_{M'})$ ,  $D = c_M^2 (f_M^2 - f_{M'}^2)$  and  $E = A + B + C + D$ .  $f_M$  and  $f_{M'}$  are the  $k$ -independent neutron scattering lengths of the isotopically distinct cations, M and M'. At the second level it is possible to determine the cation–cation structure factor,  $S_{MM}(k)$ , and hence its Fourier transform,  $g_{MM}(r)$ , from independent measurements on three isotopically enriched samples.

The same procedures are not possible with x-ray diffraction. The x-ray atomic form factors,  $f_{\alpha}(k)$ , depend on  $k$ . Fourier transformation of  $F_X(k)$  will therefore involve convolutions of the partial structure factors with the corresponding  $f_{\alpha}(k)$ . Furthermore,  $f_{\alpha}(0)$  is proportional to the electron number,  $z_{\alpha}$ , and so there is no guarantee that exchange of species with different scattering properties will lead to the same structure

**Table 1.** Properties of the solutions used in the x-ray diffraction experiments.  $\rho$  = sample density ( $\text{g cm}^{-3}$ );  $\mu$  = linear absorption coefficient ( $\text{cm}^{-1}$ );  $V$  = volume of unit composition ( $\text{\AA}^3$ ).

Label	Solution	Molality	$\rho$	$\mu$	$V$
I	3.88 M $\text{NiCl}_2$ in $\text{H}_2\text{O}$	4.204	1.424	14.9	10.069
II	3.88 M $\text{MgCl}_2$ in $\text{H}_2\text{O}$	4.337	1.267	4.55	10.374
III	3.88 M $\text{NiCl}_2$ : $\text{MgCl}_2$ 50:50 in $\text{H}_2\text{O}$	4.321	1.349	9.72	10.185
I	3.88 M $\text{NiCl}_2$ in $\text{D}_2\text{O}$	3.784	1.530	14.9	10.069
II	3.88 M $\text{MgCl}_2$ in $\text{D}_2\text{O}$	3.901	1.366	4.55	10.374
I	0.44 M $\text{NiCl}_2$ in $\text{H}_2\text{O}$	0.444	1.052	2.63	9.935
II	0.44 M $\text{MgCl}_2$ in $\text{H}_2\text{O}$	0.445	1.032	1.46	9.983
III	0.44 M $\text{NiCl}_2$ : $\text{MgCl}_2$ 50:50 in $\text{H}_2\text{O}$	0.445	1.042	2.04	9.959
I	0.1 M $\text{NiCl}_2$ in $\text{H}_2\text{O}$	0.1	1.009	1.54	9.983
II	0.1 M $\text{MgCl}_2$ in $\text{H}_2\text{O}$	0.1	1.007	1.29	9.997
I	3.88 M $\text{NiBr}_2$ in $\text{H}_2\text{O}$	4.25	1.761	55.3	10.147
II	3.88 M $\text{MgBr}_2$ in $\text{H}_2\text{O}$	4.25	1.627	47.7	10.147
III	3.88 M $\text{NiBr}_2$ : $\text{MgBr}_2$ 50:50 in $\text{H}_2\text{O}$	4.25	1.694	51.5	10.147

in solution. For this reason there is no method of substitution equivalent to the isotope technique.

An early attempt to overcome this inherently difficult problem was made by Bol *et al* (1970), who developed a method based on isomorphic substitution. This enabled them to obtain a much deeper understanding of cation hydration than had previously been possible. However, because they did not carry out any independent checks of the validity of the substitutions their results remained ambiguous.

To progress further we have used a combination of x-ray and neutron diffraction experiments. The method which we now propose is based on isomorphic substitution and x-ray diffraction, but with a check of the isomorphism by comparison with the results from the formally exact difference method of neutron diffraction. Self-consistency checks are also made among the various x-ray diffraction results. Possible isomorphic pairs are chosen on the basis of existing solid and liquid state coordination data, and dynamical properties in the liquid state, as evidenced by NMR or kinetic measurements. One of the species should also be susceptible to the isotopic substitution method of neutron diffraction.

Once a possible isomorphic pair (M and M') has been selected, x-ray diffraction experiments are carried out on three equimolar solutions of the two salts. Samples I and II contain ions M and M', respectively, and sample III is a 50:50 mixture of samples I and II (table 1). The x-ray structure factors,  $F_X(k)$ , can then be determined by the procedures of Habenschuss and Spedding (1979) or Skipper (1987). Taking solutions I and II for example, the first-order difference function,  $\tilde{\Delta}_M(k)$ , can be constructed as follows;

$$\tilde{\Delta}_M(k) = F_X^I(k) - F_X^{II}(k)$$

$$\begin{aligned} \tilde{\Delta}_M(k) = & A(k)[\tilde{S}_{MO}(k) - 1] + B(k)[\tilde{S}_{MH}(k) - 1] \\ & + C(k)[\tilde{S}_{MX}(k) - 1] + D(k)[\tilde{S}_{MM}(k) - 1] \end{aligned}$$

where

$$A(k) = 2c_{\text{O}}c_{\text{M}}f_{\text{O}}(k)\Delta f_{\text{M}}(k) \quad B(k) = 2c_{\text{H}}c_{\text{M}}f_{\text{H}}(k)\Delta f_{\text{M}}(k)$$

$$C(k) = 2c_{\text{X}}c_{\text{M}}f_{\text{X}}(k)\Delta_{\text{M}}(k) \quad D(k) = c_{\text{M}}^2\Delta^2 f_{\text{M}}(k)$$

and

$$\Delta f_{\text{M}}(k) = f_{\text{M}}(k) - f_{\text{M}'}(k)$$

and

$$\Delta^2 f_{\text{M}}(k) = f_{\text{M}}^2(k) - f_{\text{M}'}^2(k).$$

As mentioned above, the atomic form factors for x-ray diffraction,  $f_{\alpha}(k)$ , are  $k$ -dependent. Fourier transformation of equation (5) therefore results in a convoluted distribution function. However, the main aim of a first-order difference analysis is to determine the ion-water structure.  $\tilde{\Delta}_{\text{M}}(k)$  can therefore be divided by  $A(k)$  to give a new function,  $\tilde{\Delta}_{\text{MO}}(k)$ . This step enables the ion-oxygen term to be deconvoluted, and therefore allows the coordination sphere to be investigated;

$$\tilde{\Delta}_{\text{MO}}(k) = \tilde{\Delta}_{\text{M}}(k)/[2c_{\text{O}}c_{\text{M}}f_{\text{O}}(k)\Delta f_{\text{M}}(k)]$$

$$\tilde{\Delta}_{\text{MO}}(k) = [\tilde{S}_{\text{MO}}(k) - 1] + B(k)/A(k)[\tilde{S}_{\text{MH}}(k) - 1] + C(k)/A(k)[\tilde{S}_{\text{MX}}(k) - 1] + D(k)/A(k)[\tilde{S}_{\text{MM}}(k) - 1] \quad (6)$$

where

$$\tilde{S}_{\text{M}\alpha}(k) = S_{\text{M}\alpha}(k) - \{[S_{\text{M}'\alpha}(k) - S_{\text{M}\alpha}(k)][f_{\text{M}'}(k)/(f_{\text{M}}(k) - f_{\text{M}'}(k))\}$$

and

$$\tilde{S}_{\text{MM}}(k) = S_{\text{MM}}(k) - \{[S_{\text{M}'\text{M}'}(k) - S_{\text{MM}}(k)][f_{\text{M}'}^2(k)/(f_{\text{M}}^2(k) - f_{\text{M}'}^2(k))\}$$

because  $S_{\text{M}\alpha}(k)$  and  $S_{\text{M}'\alpha}(k)$  will not be identical if M and M' are not perfect isomorphs. The corresponding distribution function is then

$$\tilde{G}_{\text{MO}}(r) = [\tilde{g}_{\text{MO}}(r) - 1] + 1/(2\pi^2\rho r) \int_0^{\infty} \{B(k)/A(k)[\tilde{S}_{\text{MH}}(k) - 1] + C(k)/A(k)[\tilde{S}_{\text{MX}}(k) - 1] + D(k)/A(k)[\tilde{S}_{\text{MM}}(k) - 1]\} \sin(kr) k \, dk$$

$$\tilde{G}_{\text{MO}}(r) = \tilde{g}_{\text{MO}}(r) - [A(0) + B(0) + C(0) + D(0)]/A(0) + \int \{H_{\text{B,A}}|(r-r')|\tilde{g}_{\text{MH}}(r') + H_{\text{C,A}}|(r-r')|\tilde{g}_{\text{MX}}(r') + H_{\text{D,A}}|(r-r')|\tilde{g}_{\text{MM}}(r')\} \, dr' \quad (7)$$

where

$$\tilde{g}_{\alpha\beta}(r) = g_{\alpha\beta}(r) - \int_{-\infty}^{\infty} [g_{\alpha'\beta}(r) - g_{\alpha\beta}(r)]H_{f',f-f}|(r-r')| \, dr' \quad (8)$$

and  $\alpha$  is the stronger scatterer. The terms  $H_{\text{X,Y}}(r)$  in equation (7) are given by,

$$H_{\text{X,Y}}(r) = (2/\pi) \int_{-\infty}^{\infty} [X(k)/Y(k)] \cos(kr) \, dk \quad (9)$$

The effects of these functions on  $\tilde{G}_{\text{MO}}(r)$  have been discussed by Skipper (1987). In general the peak shapes may be changed by the convolution process, but their positions are not.

If the ion–oxygen peak is isolated in  $r$ -space the coordination number of oxygen around the ion,  $n_{MO}$ , can be obtained;

$$\bar{n}_{MO} = 4\pi\rho c_O \int_{r_1}^{r_2} \bar{G}_{MO}(r)r^2 dr \quad (10)$$

and so from equation (8),

$$\bar{n}_{MO} \approx n_{MO} - (n_{M'O} - n_{MO})[f_{M'}(0)/(f_M(0) - f_{M'}(0))] \quad (11)$$

where  $\bar{n}_{MO}$  is the coordination number measured by an x-ray difference experiment, and  $n_{MO}$  is the true value. The assumption involved in equation (11) is that either the species M and M' are very nearly isomorphic, or that  $H_{F,f-f}(r)$  is a good approximation to a delta function,  $\delta(r)$ .

The validity of a given isomorphic substitution can be tested in a number of ways, the most sensitive of which involve the properties of the difference functions,  $\bar{G}_{MO}(r)$ . As mentioned in § 2.2 there are two ways in which this is done in the present work. The first is to compare the x-ray difference function,  $\bar{G}_{MO}(r)$ , with the result obtained from neutron diffraction,  $G_M(r)$ . If the nearest neighbour cation–oxygen correlation in these two functions is found to be the same, within error, this is taken as proof of isomorphism.

A second means of checking isomorphism is to compare the two independent  $\bar{G}_{MO}(r)$ , which can be obtained if three  $F_X(k)$  are measured for a given system. These distribution functions will only be self-consistent if the two species M and M' are structurally isomorphic. This test is particularly valuable if it is not easy to isolate  $g_{MO}(r)$  in the neutron first-order difference function,  $G_M(r)$ . This may be the case for more weakly hydrated cations, when the nearest-neighbour peaks in  $g_{MO}(r)$  and  $g_{MH}(r)$  overlap to some extent.

It is straightforward to show that if x-ray diffraction measurements are made on three solutions (including a 50:50 mixture of the two original samples) then a second-order difference function can be constructed to give  $\bar{S}_{MM}(k)$  directly;

$$\bar{S}_{MM}(k) - 1 = \bar{\Delta}_M^1/A'(k) - \bar{\Delta}_M^2/B'(k) \quad (12)$$

where  $\bar{\Delta}_M^1(k) = F_X^I(k) - F_X^{II}(k)$ ,  $\bar{\Delta}_M^2(k) = F_X^I(k) - F_X^{III}(k)$  and  $A'(k) = c_M^2\{f_M^I(k) - f_M^{II}(k)\}\{f_M^I(k) - f_M^{III}(k)\}$ ,  $B'(k) = c_M^2\{f_M^I(k) - f_M^{III}(k)\}\{f_M^{II}(k) - f_M^{III}(k)\}$  and  $f_M^I(k) = f_M(k)$ ,  $f_M^{II}(k) = f_{M'}(k)$  and  $f_M^{III}(k) = [f_M(k) + f_{M'}(k)]/2$ .

The distribution function associated with the second-order difference intensity is,

$$\bar{g}_{MM}(r) = 1 + 1/(2\pi^2\rho r) \int_0^\infty [\bar{S}_{MM}(k) - 1] \sin(kr)k dk \quad (13)$$

It is worth pointing out that equation (12) gives  $\bar{S}_{MM}(k)$  exactly within the limits of the isomorphic substitution, if the various  $f_\alpha(k)$  are known.

Once isomorphism has been established at the level of a first-order difference, a second-order difference analysis can be expected to produce reliable cation–cation distributions. This is based on the assertion that as a result of screening by the solvent, chemical differences between the ions will have more effect on cation–water than cation–cation interactions. Conditions should therefore be chosen to make the formation of stable ion pairs unlikely. In particular, the use of very concentrated solutions (>4 m) or strongly nucleophilic anions should be avoided.

### 3. Experimental procedures

#### 3.1. Sample preparation

All samples were prepared under glove box conditions in our chemical laboratory at Bristol (table 1). The deuterated solutions used in the neutron diffraction experiments were checked for light water content using infra-red spectrometry, and their isotopic content was determined by mass spectrometry. Apart from the heavy water solutions used to check the isomorphism, all other samples were made with de-ionised water.

#### 3.2. Diffraction experiments

The neutron diffraction experiments of Neilson and Enderby (1978, 1983) were carried out under ambient conditions on the D4B diffractometer of the ILL, Grenoble. Neutrons of wavelength  $0.7 \text{ \AA}$  were scattered by two isotopically enriched samples;  $^{\text{N}}\text{NiCl}_2$  and  $^{62}\text{NiCl}_2$  in  $\text{D}_2\text{O}$ . The data were corrected by standard methods for absorption, multiple scattering and incoherent scattering and then normalised to give the structure factors of the solutions (Soper *et al* 1977). The difference function,  $\Delta_{\text{M}}(k)$ , was calculated from the two structure factors,  $F_{\text{N}}(k)$ , and its Fourier transform,  $G_{\text{M}}(r)$ , was used to obtain a real-space representation of the structure around  $\text{Ni}^{2+}$ . The nearest-neighbour  $\text{Ni}^{2+}\text{-O}$  correlation of  $G_{\text{M}}(r)$  was used to test the validity of the substitution of  $\text{Mg}_{[\text{aq}]^{2+}}$  for  $\text{Ni}_{[\text{aq}]^{2+}}$ .

The x-ray diffraction experiments were carried out in reflection geometry on a  $\theta\text{-}\theta$  x-ray diffractometer, manufactured by Rigaku Corporation of Tokyo. The arrangement was very similar to that employed by Levy *et al* (1965), and used an approximation to Bragg/Brentano para-focusing in which the sample was flat. In this geometry both the x-ray source and detector arms subtended an angle  $\theta$  to the free surface of the liquid sample.

X-rays of wavelength  $0.7107 \text{ \AA}$  were produced by an Mo target x-ray tube, operated at 50 kV and 40 mA. To remove the  $\text{MoK}_{\beta}$  radiation, of wavelength  $0.672 \text{ \AA}$ , a  $0.075 \text{ mm}$  Zr filter was placed in the incident beam. If this is not done the  $\text{K}_{\beta}$  radiation can contribute to the measured Compton intensity at large scattering angles. A focusing graphite monochromator was placed in the reflected beam to reduce the Compton intensity and background radiation.

The sample holders were sealed cylindrical tubes of diameter at least 10 cm, clamped so the longitudinal axis was perpendicular to the plane of the source and detector arms. A semi-circular window was cut in the container, to present a uniform surface of at least 8 cm to the incident beam. The material used was either brass coated in 'araldite' or glass, and the window was covered by aluminium foil or 'cling film', or both. The seal was made with vacuum grease, and the level of the liquid was adjusted by a 10 ml syringe.

The height of the sample was set to maximise the detected count rate at  $2\theta = 14^\circ$ , this angle being chosen to coincide with the maximum scattered intensity of most aqueous samples. It was estimated that the level adjustment was accurate to within  $\pm 0.03 \text{ mm}$ . The horizontal width of the incident beam was reduced to the dimensions of the container window by a 1 mm thick lead template. This helped to control container scattering.

Data were collected over the range  $2^\circ < 2\theta < 156^\circ$ , which corresponds to  $0.3 \text{ \AA}^{-1} < k < 17.5 \text{ \AA}^{-1}$ . The step size,  $\Delta\theta$ , was chosen so that  $\Delta k < 0.03 \text{ \AA}^{-1}$ . The total number of counts at any angle varied between 75 000 and 600 000, with the counting time being chosen so that the statistical error in  $kI(k)$  was fairly constant, and below

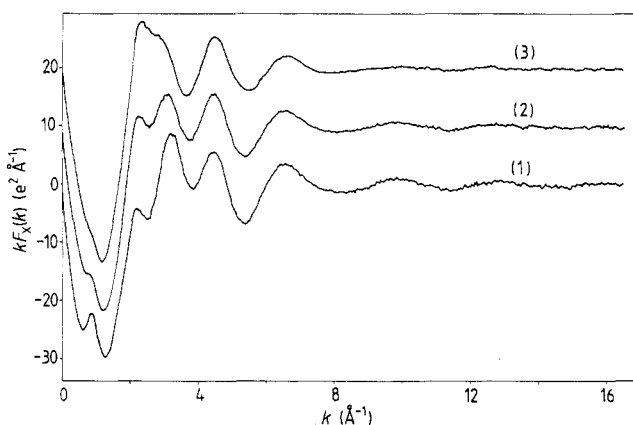


**Figure 1.** X-ray structure factors,  $kF_X(k)$ , for 3.88 M  $\text{NiCl}_2$  (curve 1), 3.88 M  $\text{MgCl}_2$  (curve 3, displaced by  $20 \text{ e}^2 \text{ \AA}^{-1}$ ) and a 50:50 mixture of  $\text{NiCl}_2$  and  $\text{MgCl}_2$  (curve 2, displaced by  $10 \text{ e}^2 \text{ \AA}^{-1}$ ).

0.5%. The data were analysed by the methods of Skipper (1987) and Habenschuss and Spedding (1979) to give normalised  $F_X(k)$ .

## 4. Results and discussion

### 4.1. Demonstration of the isomorphism between $\text{Ni}_{[\text{aq}] }^{2+}$ and $\text{Mg}_{[\text{aq}] }^{2+}$

Nickel is a d-block element, and its experimentally measured hydration enthalpy,  $\Delta H_E = -2105 \text{ kJ mol}^{-1}$ , is about 5% greater than the value calculated by neglecting the ligand field stabilisation energy,  $\Delta H_C = -1979 \text{ kJ mol}^{-1}$  (Parrish 1977). Comparison of these values with  $\Delta H_E$  for  $\text{Mg}^{2+}$ ,  $1921 \text{ kJ mol}^{-1}$ , shows that the chemical differences between the ions accounts for about 10% of the total hydration energy. This is reflected in the average lifetimes of water molecules coordinated to the two ions, which are about  $4 \times 10^{-4} \text{ s}$  and  $2 \times 10^{-6} \text{ s}$  for  $\text{Ni}^{2+}$  and  $\text{Mg}^{2+}$ , respectively (Friedman 1985). However, it is possible for the two ions to be structural isomorphs, because the structural averages of a statistical system are independent of both the masses of the constituents, and the absolute energy.

Previous structural information has shown that within the experimental errors the nearest-neighbour cation–oxygen distance ( $r_{\text{MO}}$ ) and coordination number ( $n_{\text{MO}}$ ) are  $2.07 \text{ \AA}$  and 6.0 respectively for both  $\text{Ni}^{2+}$  and  $\text{Mg}^{2+}$  (Huheey 1975, Neilson and Enderby 1978, 1979, 1983, Shannon and Prewitt 1969). The isomorphism of  $\text{Ni}_{[\text{aq}] }^{2+}$  and  $\text{Mg}_{[\text{aq}] }^{2+}$  in concentrated chloride solutions has been confirmed in the preliminary work of Skipper *et al* (1986). For completeness we now present a detailed discussion of the results of this earlier study, and make further use of the method.

X-ray diffraction data were gathered on five solutions;— three were in light water (3.88 M  $\text{NiCl}_2$ , 3.88 M  $\text{MgCl}_2$  and a 50:50 mixture of 3.88 M  $\text{NiCl}_2$  and 3.88 M  $\text{MgCl}_2$ ) and two were in heavy water (3.88 M  $\text{NiCl}_2$  and 3.88 M  $\text{MgCl}_2$ ). The data were analysed by the methods discussed in § 3.2, and the structure factors were determined (figure 1). On the assumption that  $\text{Ni}_{[\text{aq}] }^{2+}$  and  $\text{Mg}_{[\text{aq}] }^{2+}$  are isomorphous the first-order difference



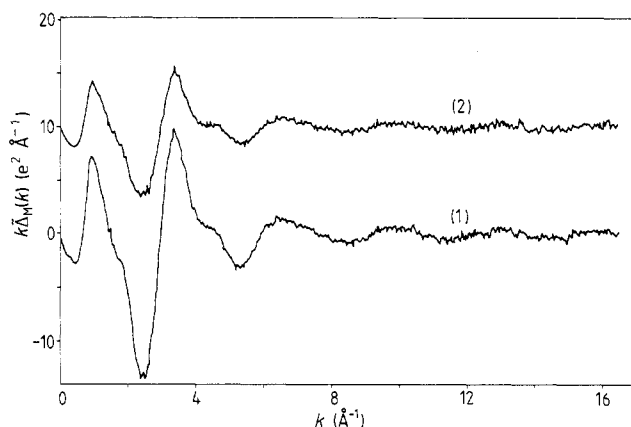


**Figure 2.** First-order difference functions,  $k\bar{\Delta}_M(k)$ , for 3.88 M Ni/MgCl<sub>2</sub> (see table 1). The results for solutions [I-II] are shown in curve 1 and those for solutions [III-II] in curve 2 (displaced by  $10 e^2 \text{Å}^{-1}$ ).

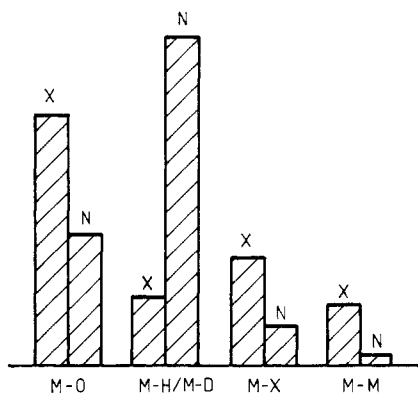


**Figure 3.** Relative weightings at  $k = 0$  of the correlations in the x-ray (X) and neutron (N) difference functions,  $\Delta_M(k)$  and  $\bar{\Delta}_M(k)$ .  $\Delta_M(k)$  is for  $^{61}\text{Ni}$  and  $^{62}\text{Ni}$  isotopes in 4.35 m NiCl<sub>2</sub> in D<sub>2</sub>O, and  $\bar{\Delta}_M(k)$  is for Ni<sup>2+</sup> and Mg<sup>2+</sup> isomorphs in 3.88 M NiCl<sub>2</sub> and MgCl<sub>2</sub> in H<sub>2</sub>O.

functions,  $\bar{\Delta}_M(k)$ , of the two sets of solutions were determined (figure 2). At this stage it is worth indicating the relative contributions to  $\bar{\Delta}_M(k)$  and  $\Delta_M(k)$ , to show that the correlations  $S_{MO}(k)$  and  $S_{MD}(k)$  dominate these functions. As shown in figure 3 this is the case.

The functions  $\tilde{G}_{MO}(r)$  for both the light and heavy water solutions are shown in figure 4. The properties of these distributions are summarised in table 2, where the quoted errors are related to the size of the unphysical oscillations between 1.5 Å and 2.0 Å. As a preliminary check of the isomorphism between Ni<sub>[aq]</sub><sup>2+</sup> and Mg<sub>[aq]</sub><sup>2+</sup> it is noted that the two independent  $\tilde{G}_{MO}(r)$  for the light water solutions are self-consistent. The sensitivity of this test has been discussed by Skipper (1987). There is no significant difference between the  $\tilde{G}_{MO}(r)$  obtained from solutions in light and heavy water.

A more stringent test of the isomorphism is obtained by comparing the x-ray result,  $\tilde{G}_{MO}(r)$ , with the neutron result of Neilson and Enderby (1978),  $G_M(r)$ , and focusing attention on the nearest neighbour metal–oxygen correlation. As can be seen in figure

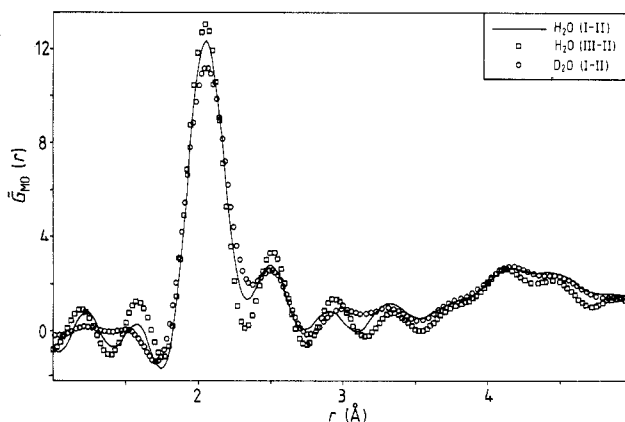


**Figure 4.** X-ray first-order difference distribution function,  $G_M(r)$ , for 3.88 M Ni/MgCl<sub>2</sub> solutions (table 1). The distributions obtained from the solutions in H<sub>2</sub>O are the solid line (solutions [I-II]) and the squares (solutions [III-II]). The distribution obtained from the solutions in D<sub>2</sub>O is given by the circles.

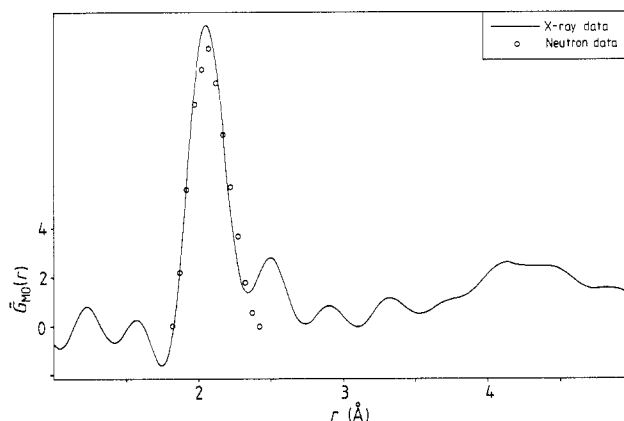


**Figure 5.** X-ray first-order difference distribution,  $\tilde{G}_{MO}(r)$ , for 3.88 M NiCl<sub>2</sub> and MgCl<sub>2</sub> in H<sub>2</sub>O (full curve) compared with the nearest neighbour Ni<sup>2+</sup>-O correlation in 4.35 m NiCl<sub>2</sub>, as measured by Neilson and Enderby (1983) using the first-order difference method of neutron diffraction (circles).

5 this function is the same within error for the two data sets, and gives  $\bar{n}_{MO} = 5.9 \pm 0.2$  and  $r_{MO} = 2.06 \pm 0.02$  Å (table 2). This confirms that in concentrated chloride solutions Ni<sup>2+</sup> and Mg<sup>2+</sup> can be regarded as isomorphic species with respect to the local oxygen coordination. Since Neilson and Enderby (1983) have shown that there is no significant penetration of Cl<sup>-</sup> into the coordination sphere of Ni<sup>2+</sup>, even in 4.35 m NiCl<sub>2</sub> solutions, it is concluded that Ni<sup>2+</sup> and Mg<sup>2+</sup> will be isomorphic in any concentration of chloride solution. The case of other anions is discussed in § 4.3.

No quantitative analysis was carried out for the M-H or M-D correlations, because these terms are very weak when measured by x-ray diffraction. It should be pointed out, however, that the nearest-neighbour M-H separation is shorter when measured by x-ray diffraction, but that this is not inconsistent with isomorphism (Skipper 1987). Water molecules in the hydration sphere are polarised to some extent by the cation, and so the

**Table 2.** Properties of the radial distribution functions obtained by x-ray and neutron diffraction experiments on aqueous NiCl<sub>2</sub> and NiBr<sub>2</sub>.  $r_{\text{NiO}}$  = peak position of the nearest-neighbour Ni–O correlation (Å);  $r_{\text{NiH}}$  = peak position of the nearest-neighbour N–H of Ni–D correlation (Å);  $n_{\text{NiO}}$  = coordination number for the nearest neighbour Ni–O correlation;  $\Delta r_{\text{NiO}}$  = half height width of the nearest-neighbour Ni–O correlation (Å). An indication of the errors in the last digit are given in parentheses. Neutron data were taken from Neilson and Enderby (1978).

Solution	Probe	$r_{\text{NiO}}$	$r_{\text{NiH}}$	$n_{\text{NiO}}$	$\Delta r_{\text{NiO}}$	Solvent	Difference
4 M NiCl <sub>2</sub>	Neutrons	2.07(2)	2.67(2)	5.8(2)	0.26(2)	D <sub>2</sub> O	
3.88 M NiCl <sub>2</sub>	X-rays	2.06(2)	2.51(2)	5.9(2)	0.24(2)	D <sub>2</sub> O	
3.88 M NiCl <sub>2</sub>	X-rays	2.06(2)	2.50(2)	5.9(2)	0.23(2)	H <sub>2</sub> O	[I–II]
		2.06(2)	2.50(2)	6.0(2)	0.22(2)	H <sub>2</sub> O	[III–II]
3.88 M NiBr <sub>2</sub>	X-rays	2.06(4)	2.56(6)	5.6(4)	0.27(4)	H <sub>2</sub> O	[I–II]
		2.08(4)	2.56(6)	5.8(4)	0.25(4)	H <sub>2</sub> O	[III–II]
0.44 M NiCl <sub>2</sub>	X-rays	2.07(2)	2.61(4)	6.0(4)	0.23(6)	H <sub>2</sub> O	[I–II]
		2.06(2)	2.70(8)	5.6(8)	0.21(8)	H <sub>2</sub> O	[III–II]
0.4 M NiCl <sub>2</sub>	Neutrons	2.10(2)	2.80(2)	6.8(9)	0.37(5)	D <sub>2</sub> O	
0.1 M NiCl <sub>2</sub>	X-rays	2.06(6)	2.50(8)	5.6(10)	0.20(10)	H <sub>2</sub> O	

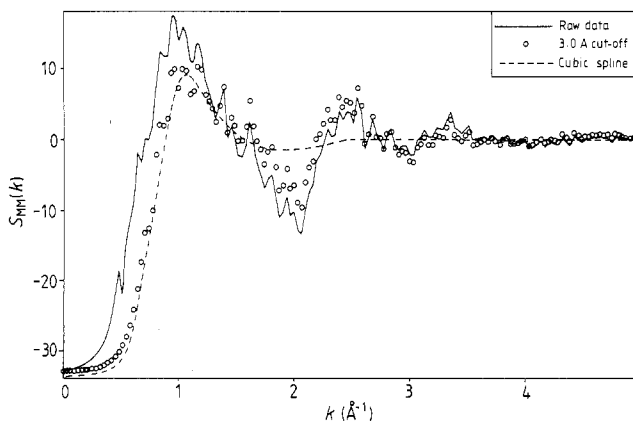


**Figure 6.** The function  $\tilde{S}_{\text{MM}}(k)$  in 3.88 M Ni/MgCl<sub>2</sub> in H<sub>2</sub>O measured by the second-order difference method of x-ray diffraction. The solid line is the raw data multiplied by  $e^{-0.05k^2}$ , the circles show the result of cutting  $\tilde{g}_{\text{MM}}(r)$  off at 3.0 Å and back Fourier transformation and the dashed line is a cubic spline fit to the circles. To obtain this fit the knots were placed at 0.4, 0.8, 1.2, 1.6, 2.8 and 4.0 Å<sup>-1</sup>. This selection is based on the assumption that there will be little real structure beyond 2 Å<sup>-1</sup> (Friedman and Dudowicz 1980).

centres of negative charge (measured by x-rays) will not coincide with the centres of positive charge (measured by neutrons) for these molecules.

On the assumption of isomorphism a second-order difference function can be constructed, which gives  $\tilde{S}_{\text{MM}}(k)$  directly (equation 12). The result for 3.88 M Ni/MgCl<sub>2</sub> is shown as the solid line in figure 6. This function is multiplied by  $e^{-0.05k^2}$  and extrapolated to  $-33.6$  (Beeby 1973). It is compared with the neutron diffraction result of Neilson and Enderby (1983) in figure 7. The Fourier transform of the x-ray data,  $\tilde{g}_{\text{MM}}(r)$ , exhibits a residual M–O peak at 2.06 Å, which is probably a result of normalisation errors in the difference functions,  $\tilde{\Delta}_{\text{M}}(k)$ . The result of setting  $\tilde{g}_{\text{MM}}(r)$  to zero below 3 Å and then

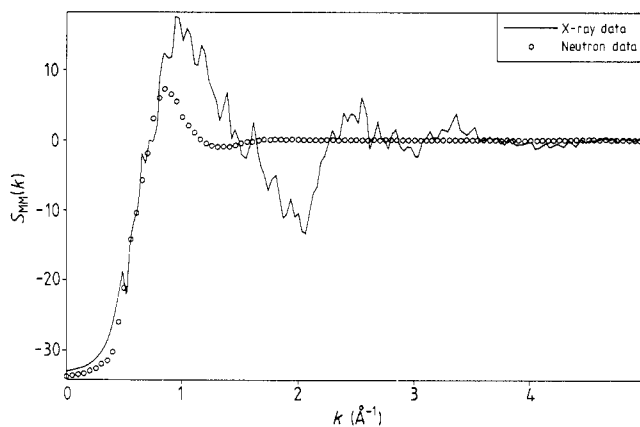


**Figure 7.** Comparison of the  $S_{MM}(k)$  measured by x-ray and neutron diffraction. The solid line is the raw x-ray data and the circles are the smoothed neutron data of Neilson and Enderby (1983).

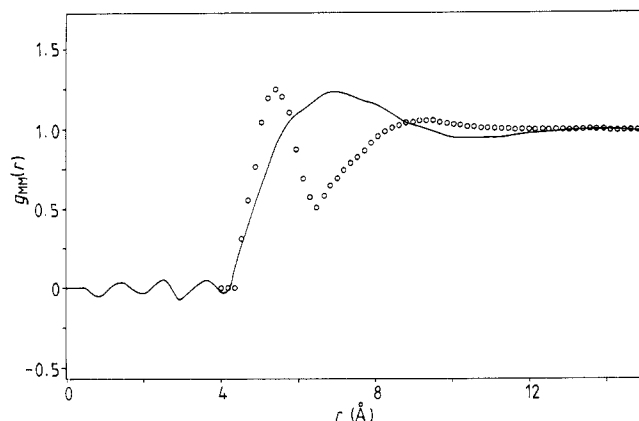


**Figure 8.** Comparison of  $\tilde{g}_{MM}(r)$  for 3.88 M Ni/MgCl<sub>2</sub> measured by x-ray diffraction (solid line) with  $g_{MM}(r)$  for 4.35 M NiCl<sub>2</sub> measured by neutron diffraction (circles).

back Fourier transformation is shown as the circles in figure 6. A final  $\tilde{S}_{MM}(k)$  was obtained from this function by smoothing, and is the dashed line in figure 6. The corresponding  $\tilde{g}_{MM}(r)$  is shown in figure 8, along with the neutron result.

The positions of the cut-off and first peak ( $r_{co}$  and  $r_p$ ) in the smoothed x-ray  $\tilde{g}_{MM}(r)$  are  $3.8 \pm 0.5 \text{ \AA}$  and  $7.0 \pm 1.0 \text{ \AA}$ , respectively. As a result of systematic errors present in the original  $\tilde{S}_{MM}(k)$ , it is difficult to quantify the uncertainties in the final  $\tilde{g}_{MM}(r)$ ; the bounds quoted for  $r_c$  and  $r_p$  represent the confidence limits of the fitted data.

As a result of the increased weighting of the M–M term in the x-ray data (see figure 3) we feel that  $\tilde{S}_{MM}(k)$  derived from the x-ray studies is more closely representative of the true  $S_{MM}(k)$  of the solution. We draw attention to the fact that the smoothed  $\tilde{g}_{MM}(r)$  derived from our x-ray diffraction experiments does not exhibit the peak at  $r_p = 4.7 \text{ \AA}$ , which is present in the neutron data. However, the  $g_{MM}(r)$  derived from the x-ray and neutron and x-ray studies cut off at about the same value,  $r_{co} \approx 4 \text{ \AA}$ . The x-ray curve is

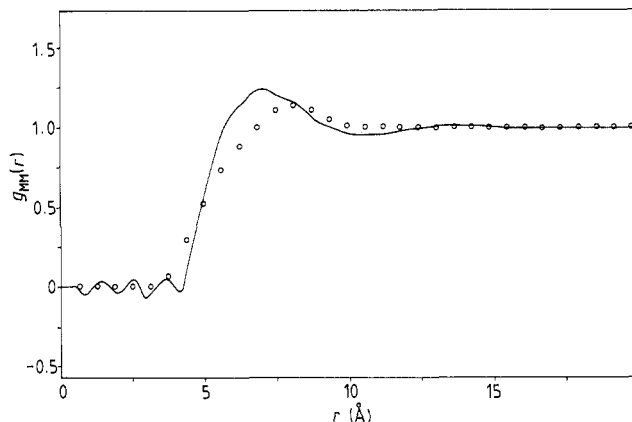


**Figure 9.** Comparison of  $\bar{g}_{MM}(r)$  for 3.88 M Ni/MgCl<sub>2</sub> measured by x-rays (solid line) with the theoretical  $\bar{g}_{MM}(r)$  for 4 M NiCl<sub>2</sub> calculated by Friedman and Dudowicz (1980) (circles).

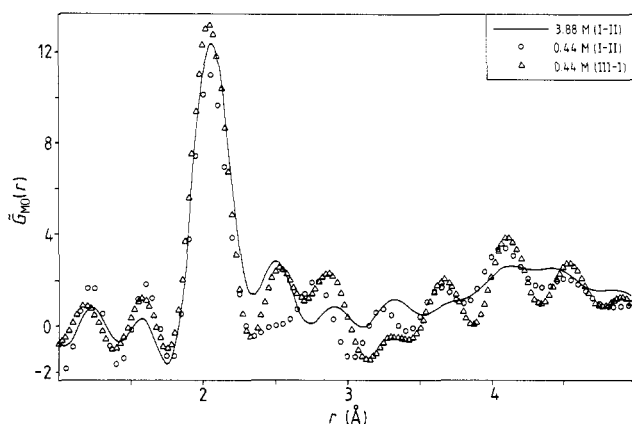


**Figure 10.**  $\bar{G}_{MO}(r)$  for 0.44 M Ni/MgCl<sub>2</sub> compared with the result for 3.88 M Ni/MgCl<sub>2</sub>. The full curve is for the 3.88 M Ni/Cl<sub>2</sub> (solutions [I-II]) and the circles and triangles are for the 0.44 M Ni/MgCl<sub>2</sub> (solutions [I-II] and [III-II] respectively).

compared with the theoretical prediction of Friedman and Dudowicz (1980) in figure 9 (see § 4.4).

Having demonstrated that Ni<sup>2+</sup> and Mg<sup>2+</sup> are isomorphic in concentrated chloride solutions, we exploit this observation by studying Ni<sup>2+</sup>/Mg<sup>2+</sup> coordination as a function of concentration and counter-ion.

#### 4.2. Concentration dependence of Ni<sub>[aq]</sub><sup>2+</sup>/Mg<sub>[aq]</sub><sup>2+</sup> coordination

X-ray diffraction data were gathered for 0.4 M and 0.1 M NiCl<sub>2</sub> and MgCl<sub>2</sub> solutions (table 1). The distribution functions,  $\bar{G}_{MO}(r)$ , obtained from these solutions are shown in figures 10 and 11. There are two points which can be made regarding these results. The first is that the nearest-neighbour cation–oxygen peaks give results which are consistent with those obtained in neutron studies (table 2). The second is that the results for the 0.1 M solution are at the limit of the present technology. Experiments on such

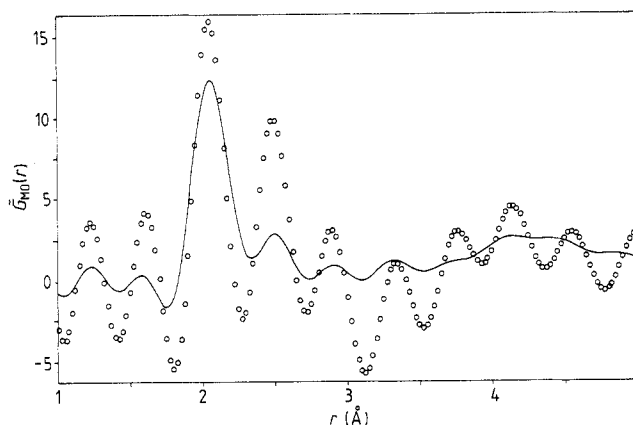


Figure 11.  $\tilde{G}_{\text{MO}}(r)$  for 0.1 M Ni/MgCl<sub>2</sub> (circles) compared with the result for 3.88 M Ni/MgCl<sub>2</sub> (full curve).

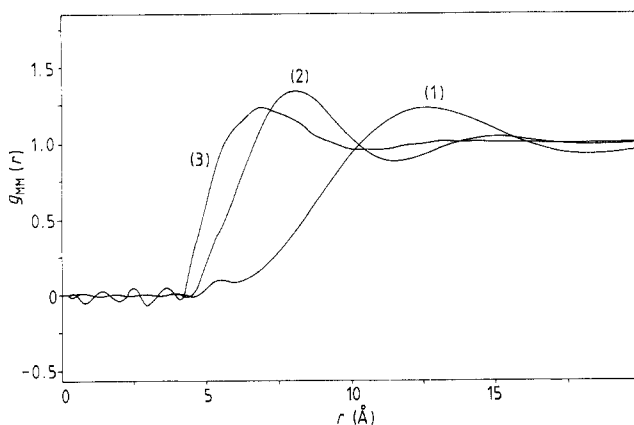
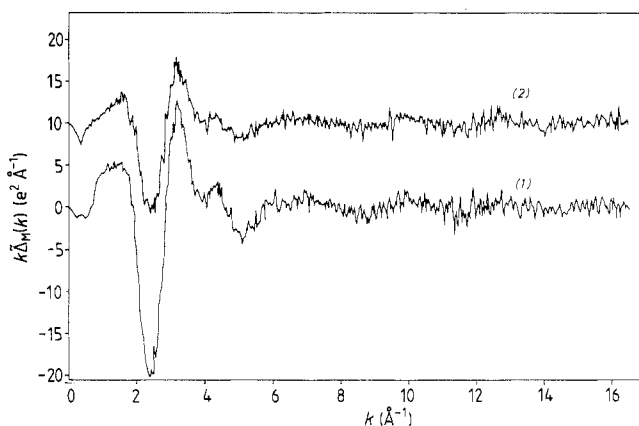


Figure 12. Smoothed  $\tilde{g}_{\text{MM}}(r)$  measured by x-ray diffraction, for 0.44 M NiCl<sub>2</sub> (curve 1), 3.88 M NiBr<sub>2</sub> (curve 2) and 3.88 M NiCl<sub>2</sub> (curve 3).

dilute solutions should, however, be feasible with a synchrotron source, which produces a flux several orders of magnitude greater than those obtained from laboratory sources.

The results for the first order differences are summarised in table 2. From these values it is concluded that in the concentration range studied there is no measurable change in either the position ( $r_{\text{MO}}$ ), coordination number ( $\bar{n}_{\text{MO}}$ ) or half-height width ( $\Delta r_{\text{MO}}$ ) of the nearest-neighbour oxygen correlation around  $\text{Ni}^{2+}$  and  $\text{Mg}^{2+}$ .

A second-order difference analysis was attempted for the 0.4 M solutions. This represents the limit of the present x-ray set, and the combination of statistical and normalisation errors in the first-order difference functions made it necessary to set both  $\tilde{G}_{\text{MO}}(r)$  to zero below 3.0 Å before  $\tilde{S}_{\text{MM}}(k)$  was constructed. If this was not done a residual of the M–O peak at 2.06 Å dominated the M–M correlations. The raw  $\tilde{S}_{\text{MM}}(k)$  was smoothed and Fourier transformed to give the distribution  $\tilde{g}_{\text{MM}}(r)$ , which is shown in figure 12. The positions of the cut-off ( $r_c$ ) and first peak ( $r_p$ ) in this function occurred at  $4.5 \pm 1.0$  Å and  $12.5 \pm 2.0$  Å, respectively. Throughout the second-order analysis  $k$ -space data were multiplied by  $e^{-0.05k^2}$ , and  $\tilde{S}_{\text{MM}}(0)$  was taken as  $-150.0$ , to give a



**Figure 13.**  $k \Delta_M(r)$  for 3.88 M NiBr<sub>2</sub>. Curve 1 is from solutions [I–II] and curve 2 is from solutions [III–II] (table 1).

reasonable extrapolation to the first usable datum point at  $0.6 \text{ \AA}^{-1}$ . The results suggest that  $\tilde{g}_{MM}(r)$  has approximately the same shape as in the 3.88 M case, but that  $r_p$  is displaced to larger  $r$  on dilution.

#### 4.3. Anion dependence of $M^{2+}$ hydration and of $M^{2+}$ – $M^{2+}$ coordination in concentrated $Ni^{2+}/Mg^{2+}$ salt solutions

As shown in § 4.1,  $Ni_{[aq]}^{2+}$  and  $Mg_{[aq]}^{2+}$  can be regarded as structural isomorphs in chloride solutions, but this does not necessarily mean that the pair will be isomorphous in the presence of other anions. To investigate the case of simple halide solutions the experiments of § 4.1 were repeated, replacing  $Cl^-$  for  $Br^-$ . This substitution was chosen for the following reasons.

It has been reported that in concentrated NiBr<sub>2</sub> solutions a significant number of bromide ions displace water in the coordination sphere of the cation (Magini *et al* 1985). Since bromide ions are strong scatterers of x-rays ( $z_{Br^-} = 36$ ,  $z_{Cl^-} = 18$ ) the difference method is suited to measure this displacement effect. In contrast to this it is improbable that x-ray diffraction techniques would be able to detect the presence of either  $F^-$  or  $I^-$  coordination sphere of  $Ni^{2+}$  and  $Mg^{2+}$ .  $F^-$  is a weak scatterer of x-rays ( $z_{F^-} = 10$ ), and it is unlikely that a significant number of cation–anion pairs form in NiI or MgI solutions, since the stability of halide complexes with  $Ni_{[aq]}^{2+}$  or  $Mg_{[aq]}^{2+}$  decreases in the order  $F^- > Cl^- > Br^- > I^-$  (Cotton and Wilkinson 1972).

The x-ray diffraction procedures of § 4.1 were repeated on three solutions of 3.88 M Ni/MgBr<sub>2</sub> (table 1) and the functions  $F_X(k)$  were determined. Compared with the results for the Ni/MgCl<sub>2</sub> solutions there was a significant increase in the magnitude of the statistical errors (see figures 2 and 13). This was caused by the large linear absorption coefficients of the solutions (about  $50 \text{ cm}^{-1}$  for  $\lambda = 0.7 \text{ \AA}$ ), which reduced the measured count rates by a factor of at least ten compared with the chloride samples. Due to the small instabilities of the x-ray tube when operated over long periods increased counting times would not have reduced the overall error.

The first-order difference functions,  $\tilde{\Delta}_M(k)$  and  $\tilde{G}_{MO}(r)$ , are shown in figures 13 and 14. The two  $\tilde{G}_{MO}(r)$  obtained from solutions [I–II] and [III–II] were consistent, and their properties are summarised in table 2. From these results it is concluded that exchanging

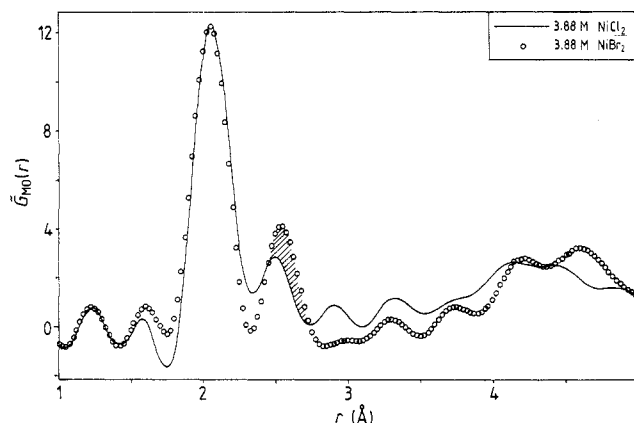


**Figure 14.**  $\tilde{G}_{\text{MO}}(r)$  for 3.88 M Ni/MgBr<sub>2</sub> (solutions [I–II], circles) and 3.88 M Ni/MgCl<sub>2</sub> (solutions [III–II], full curve); see table 1.

chloride for bromide as the anions has little effect on the coordination of  $\text{Ni}^{2+}$  or  $\text{Mg}^{2+}$  in concentrated solutions. This does not preclude the possibility of a small amount of inner sphere penetration by the anions.

$\tilde{G}_{\text{MO}}(r)$  from solutions [I–II] is compared with the corresponding function for the 3.88 M Ni/MgCl<sub>2</sub> (see figure 14). The data from solutions [III–II] were chosen for the Ni/MgCl<sub>2</sub>, since these contain statistical errors of a size closer to those of the bromide data. There is an increase in the magnitude of  $\tilde{G}_{\text{MO}}(r)$  at around  $r = 2.6$  Å for the bromide data relative to the chloride data, consistent with the presence of some  $\text{Br}^-$  in the cation coordination sphere. However, given the size of the unphysical oscillations in the distribution functions the present work is not conclusive in this respect.

The amount of  $\text{Br}^-$  in the coordination sphere of the cation was estimated in two ways. In both of these  $\tilde{\Delta}_{\text{M}}(k)$  was divided by  $C(k)$  (equation 5), to deconvolute  $\tilde{G}_{\text{M}}(r)$  with respect to the M–Br term and produce  $\tilde{G}_{\text{MBr}}(r)$ . In this function the area under the peak centred at 2.5 Å will contain contributions from both the M–H and M–Br correlations. To estimate the contribution from the M–H term, the function ' $\tilde{G}_{\text{MBr}}(r)$ ' was constructed for the 3.88 M chloride data. By taking the difference between the  $\tilde{G}_{\text{MBr}}(r)$  for the bromide and chloride data and integrating the result between  $r_1 = 2.45$  Å and  $r_2 = 2.75$  Å the shaded area in figure 14 was determined;-

$$A_{\text{Br}} = 4\pi\rho c_{\text{Br}} \int_{r_1}^{r_2} \tilde{G}_{\text{MBr}}(r)r^2 dr. \quad (14)$$

This area can be interpreted in two ways.

If it is assumed that  $\text{Cl}^-$  is absent from the inner coordination sphere of the cation in the chloride solutions, then  $\tilde{n}_{\text{MBr}^-}$  is given directly from  $A_{\text{Br}}$ . If, however,  $\text{Cl}^-$  behaves like  $\text{Br}^-$  with respect to the inner sphere, then  $\tilde{n}_{\text{MBr}^-}$  can be approximated by

$$\tilde{n}_{\text{MBr}} \approx A_{\text{Br}} [f_{\text{Br}}(0) / (f_{\text{Br}}(0) - f_{\text{Cl}}(0))]. \quad (15)$$

The two methods give  $\tilde{n}_{\text{Br}} = 0.1 \pm 0.1$  and  $\tilde{n}_{\text{Br}} = 0.2 \pm 0.2$ , respectively. Since the only direct measurement of  $g_{\text{Ni-Cl}}(r)$ , by Neilson and Enderby (1983), indicates that no  $\text{Ni}^{2+}$ – $\text{Cl}^-$  pairs are formed in 4.35 m NiCl<sub>2</sub>, the first figure is more reliable. The result of  $\tilde{n}_{\text{Br}} = 0.1 \pm 0.1$  compares with a value of  $0.44 \pm 0.06$  measured in a conventional x-ray



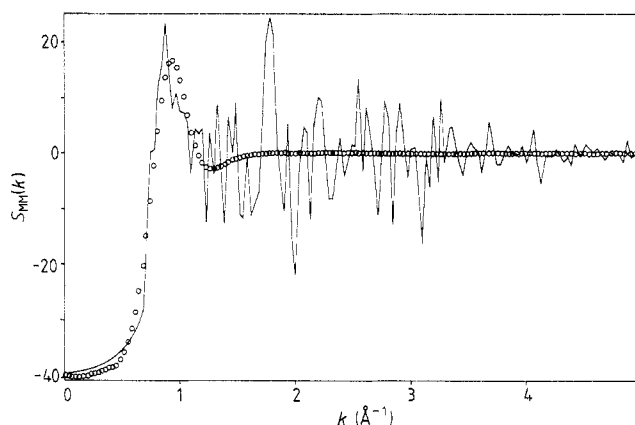


**Figure 15.**  $\tilde{S}_{MM}(k)$  for 3.88 M Ni/MgBr<sub>2</sub>, as measured by x-ray diffraction. The full curve is the raw data multiplied by  $e^{-0.05k^2}$  and the circles are a cubic spline fit to the full curve (see caption to figure 6 for details).

diffraction study by Magini *et al* (1985). The discrepancy between the two methods could arise either because Ni<sup>2+</sup> and Mg<sup>2+</sup> are not isomorphic with respect to inner-sphere bromide ions, or because the errors associated with one of the experiments have been underestimated.

The second-order difference functions,  $\tilde{S}_{MM}(k)$  and  $\tilde{g}_{MM}(r)$ , were constructed in the same way as in § 4.1, and are shown in figures 15 and 12. To give a reasonable extrapolation from the first usable datum point at  $0.6 \text{ \AA}^{-1}$ ,  $\tilde{S}_{MM}(0)$  was taken as  $-40.0$ . Since the statistical errors associated with  $\tilde{S}_{MM}(k)$  were large it was necessary to multiply this function by  $e^{-0.05k^2}$ . For this reason the values of  $r_c = 4.5 \text{ \AA}$  and  $r_p = 8.0 \text{ \AA}$  are not reliable to less than  $\pm 1.0 \text{ \AA}$  and  $\pm 2.0 \text{ \AA}$ , respectively.

#### 4.4. Discussion of $\tilde{g}_{MM}(r)$ for all of the solutions and comparison with theory

The  $\tilde{g}_{MM}(r)$  for the three sets of solutions are shown in figure 12. From our first-order difference results and those of previous neutron diffraction studies (Neilson and Enderby 1983) we infer that the diameter of the hydration spheres of Ni<sup>2+</sup> and Mg<sup>2+</sup> are  $5.3 \text{ \AA}$ . However, the measured closest approach of the ions themselves is about  $4 \text{ \AA}$ . Although the errors of the experimental data are large, it is probable that the model for the cation–cation correlation proposed by Neilson and Enderby (1983) is correct. In this, some degree of overlap or sharing of the hydrated water is envisaged, and the closest approach of the cations is found to be  $4.0 \text{ \AA}$ . It has been suggested that a staggered overlap of the hydration spheres allows them to remain intact at this separation. If this is the case the value of  $r_c$  should be independent of concentration and the type of anion. The experimental values are consistent with this model, since  $r_c = 4.5 \pm 1.0 \text{ \AA}$  for both  $0.44 \text{ M Ni/MgCl}_2$  and  $3.88 \text{ M Ni/MgBr}_2$  and  $r_c = 3.8 \pm 0.5 \text{ \AA}$  for  $3.88 \text{ M Ni/MgCl}_2$ .

The theoretical model of Friedman and Dudowicz (1980), based on soft-sphere ions and a primitive dielectric solvent, can be used to reproduce the essential features of the experimental data for the  $3.88 \text{ M Ni/MgCl}_2$  solutions (figure 9). By setting the cation diameter to  $2.4 \text{ \AA}$  and the anion diameter to  $2.86 \text{ \AA}$  good agreement with our experimental result for  $\tilde{g}_{MM}(r)$  can be obtained. In contrast, the theory of Levesque *et al* (1980) has been used to study the properties of hard-sphere ions in a dipolar solvent. The results

of this work show that cation–cation clusters form in such a system. These are not found in the real solutions studied here. It is therefore concluded that in these systems the molecular nature of the water is only relevant to the cation–cation correlations in that it determines the effective diameter and ‘softness’ of the ions. In very dilute solutions ( $<0.01$  m) the exact values of these parameters probably become less important, in which case the Debye and Huckel theory (1923) would need little improvement.

There is also interest in transitions from aqueous solution to crystal hydrate to solid salt and then to molten salt (Enderby *et al* 1987). Since the structures of the crystal hydrate  $MgCl_2 \cdot 12H_2O$  and solid and molten salts of  $MgCl_2$  are known (Sasvari and Jeffrey 1966; Biggin *et al* 1984) the present work is useful in this respect.

A striking difference is noted between the cation–cation correlations in the 3.88 M solution ( $MgCl_2 \cdot 14.3H_2O$ ) and the crystal hydrate ( $MgCl_2 \cdot 12H_2O$ ), which is stable at  $-20^\circ C$ . The maximum in the  $g_{MM}(r)$  of the liquid is at  $7.2 \text{ \AA}$ , which is the same as the nearest neighbour distance in the crystal. However, in the solution the closest approach of the cations is about  $4 \text{ \AA}$ . Such a large change is not found for the cation–anion or anion–anion terms (Enderby *et al* 1987). It may be concluded that in the hydrates the interaction between the hydrated  $Mg^{2+}$  ions is weak, as a result of the screening effect of the solvent.

## 5. Conclusions

The results presented in this paper demonstrate that as far as local oxygen coordination is concerned  $Ni^{2+}$  and  $Mg^{2+}$  can be regarded as structurally isomorphic species in aqueous solution. Application of this isomorphism to x-ray diffraction has confirmed several neutron diffraction results for cation–oxygen coordination, and enabled new information to be obtained concerning the cation–cation correlation as a function of concentration and anion type.

The coordination shell of  $Ni^{2+}$  and  $Mg^{2+}$  has been shown to contain six oxygen atoms at an average distance of  $2.06 \text{ \AA}$ . Within the limitations of the experiments these values are independent of concentration and the exchange of bromide for chloride as the counter-ion. However, the results for 3.88 M Ni/MgBr<sub>2</sub> are consistent with the penetration of  $0.1 \pm 0.1$  bromide ions into the coordination sphere of the cations.

The cation–cation correlation function,  $g_{MM}(r)$ , can be characterised by the positions of the cut-off ( $r_{co}$ ) and the centre of the first peak ( $r_p$ ). The value of  $r_{co}$  shows no significant variation for any of the solutions studied. It is  $3.8 \pm 0.5 \text{ \AA}$  for 3.88 M Ni/MgCl<sub>2</sub> and  $4.5 \pm 1.0 \text{ \AA}$  for both 3.88 M Ni/MgBr<sub>2</sub> and 0.44 M Ni/MgCl<sub>2</sub>. In contrast, the position  $r_p$  is  $7.0 \pm 1.0 \text{ \AA}$  for 3.88 M Ni/MgCl<sub>2</sub>,  $12.5 \pm 2.0 \text{ \AA}$  for 0.44 M Ni/MgCl<sub>2</sub> and  $8.0 \pm 2.0 \text{ \AA}$  for 3.88 M Ni/MgBr<sub>2</sub>.

To progress further with the method of isomorphic substitution the use of more intense x-ray beams is essential. These are available from synchrotron sources, which can produce fluxes several orders of magnitude greater than those of a conventional x-ray tube, such as that used in the present work. The use of synchrotron radiation would enable second-order difference experiments to be conducted on dilute solutions, possibly to about 0.01 M, which is the limit of the Debye and Huckel theory (Debye and Huckel 1923).

### Acknowledgments

We wish to thank the SERC for its continuing financial support of our liquids programme, and Mr P Gullidge for preparing the samples for the neutron experiments. We have also greatly benefited from discussions with Professor John Enderby.

### References

- Beeby J L 1973 *J. Phys. C: Solid State Phys.* **6** 2262  
Biggin S, Gay M and Enderby J E 1984 *J. Phys. C: Solid State Phys.* **17** 977  
Bol W, Gerrits G J A and van Panthaleon van Eck C L 1970 *J. Appl. Phys.* **3** 486  
Cotton F A and Wilkinson G 1972 *Advanced Inorganic Chemistry* 3rd edn (New York: Wiley)  
Debye and Huckel 1923 *Z. Phys.* **24** 185  
Enderby J E and Neilson G W 1981 *Rep. Prog. Phys.* **44** 38  
Enderby J E, Cummins S, Hardman J G, Neilson G W, Salmon P S and Skipper N T 1987 *J. Phys. Chem.* **91** 5851  
Friedman H L 1985 *Chem. Sci.* **25** 42  
Friedman H L and Dudowicz J B 1980 *Aust. J. Chem.* **33** 1889  
Habenschuss A and Spedding F H 1979 *J. Chem. Phys.* **70** 2797  
Huheey J E 1975 *Inorganic Chemistry* (London: Harper and Row)  
Levesque D, Weis J J and Patey G N 1980 *J. Chem. Phys.* **72** 1887  
Levy H A, Danford M D and Narten A H 1966 *Oak Ridge National Laboratory Rep.* ORNL-3960  
Magini M, de Moraes M, Licheri G and Piccaluga G 1985 *J. Chem. Phys.* **83** 5797  
Neilson G W and Enderby J E 1978 *J. Phys. C: Solid State Phys.* **11** L625  
—— 1979 *R. Soc. Chem. Ann. Rep.* C p. 185  
—— 1983 *Proc. R. Soc. Lond.* **A390** 353  
Parrish R V 1977 *The Metallic Elements* (London: Longman)  
Sasvari and Jeffrey 1966 *Acta Crystallogr.* **20** 875  
Shannon R D and Prewitt C T 1969 *Acta Cryst.* **B25** 925  
Skipper N T 1987 *PhD Thesis*, University of Bristol  
Skipper N T, Cummings S C, Neilson G W and Enderby J E 1986 *Nature* **321** 52  
Soper A K, Neilson G W, Enderby J E and Howe R A 1977 *J. Phys. C: Solid State Phys.* **10** 1793